Int. J. Heat Mass Transfer. Vol. 19, pp. 559–565. Pergamon Press 1976. Printed in Great Britain

MAXIMUM DENSITY EFFECTS ON THERMAL INSTABILITY INDUCED BY COMBINED BUOYANCY AND SURFACE TENSION

RAY-SHING WU and K. C. CHENG
Department of Mechanical Engineering, University of Alberta, Edmonton, Alberta, Canada

(*Received* 4 *July* 1975)

Abstract—Nield's linear stability analysis (1964) for a horizontal liquid layer considering surface tension and buoyancy effects is extended to the case of water with maximum density effect for the temperature range 0–30°C. Two thermal parameters (λ_1, λ_2) and three physical parameters (*Bi*, *Ra*, *Ma*) appear in the analysis. Typical results are presented for the cases involving heating from below and above.

NOMENCLATURE

A,	temperature difference ratio $(T_1 - T_{max})/\tau d$;
a,	dimensionless wave number;
Bi,	Biot number, $q_0 d/K$;
d,	liquid layer thickness;
g,	gravitational acceleration;
K,	thermal conductivity of liquid;
M,	number of divisions for liquid layer;
Ma,	Marangoni number, $\sigma_0(\Delta T)d/(\mu\alpha)$;
P,	pressure;
p,	dimensionless perturbation pressure, $P'/(\rho_0 \alpha\nu/d^2)$;
q_0,	rate of change with temperature of the time rate of heat loss per unit area from free upper surface;
Ra,	Rayleigh number, see equation (10);
T, T_1, T_2,	temperature, lower plate temperature, free surface temperature, respectively;
t,	time;
U, V, W,	perturbation velocity components in X, Y, Z directions;
u, v, w,	dimensionless perturbation velocities $(U, V, W)/(\alpha/d)$;
X, Y, Z,	rectangular coordinates;
x, y, z,	dimensionless coordinates $(X, Y, Z)/d$.

Greek symbols

α,	thermal diffusivity;
β,	coefficient of thermal expansion;
γ_1, γ_2,	temperature coefficients for density–temperature relationship;
θ,	dimensionless temperature disturbance, $\theta'/\Delta T$;
μ,	viscosity;
λ_1, λ_2,	thermal parameters defined in equation (9);
ν,	kinematic viscosity;
ρ, ρ_0,	density, reference density;
σ_0,	negative of the rate of change of surface tension with temperature;
τ,	vertical temperature gradient $(T_1 - T_2)/d$;
ΔT,	temperature difference $(T_1 - T_2) = \tau d$.

Superscripts and subscripts

$'$,	prime, perturbation quantity;
$+$,	dimensionless disturbance amplitude;
b,	quantity at unperturbed static state;
max,	value at a density maximum.

1. INTRODUCTION

IN RECENT years, experimental investigations on the onset of convection in a horizontal water layer have been reported in the literature for the thermal conditions involving both melting [1–4] and formation [1, 5] of ice. In these studies, the water layer is characterized by stable upper region and potentially unstable lower region separated by an interface with maximum density at 4°C and by continuously changing layer thickness. Theoretical studies on thermal instability of a horizontal liquid layer with maximum density have also been presented for various boundary conditions corresponding to rigid and free surfaces [6–10]. Previous theoretical and experimental investigations on thermal instability with maximum density effects are confined to Rayleigh problem only where the driving force for convection is buoyancy force. For thin horizontal liquid layers with an upper free surface, it is known that the onset of convection can be induced by surface-tension gradients [11] and buoyancy forces [12, 13].

The purpose of this study is to determine the stability criteria for the onset of cellular convection driven by surface tension and buoyancy force in a horizontal thin liquid layer by considering the density inversion effect for water using a cubic temperature–density relationship. The lower boundary is taken to be rigid and thermally conducting while at the upper free surface Pearson's boundary conditions [11, 12] are imposed to facilitate the analysis. With the maximum density effect, the liquid layer can be unstable regardless of whether heating is from below or above. The physical model in the present instability analysis is patterned after that of Nield [12]. The maximum density effect for water temperatures ranging from 0 to 30°C is of primary concern in this study. The temperature regime under consideration may be

observed under northern climatic conditions. The results of present analysis may be used in assessing the importance of cellular convection in the growth and decay of ice in contact with a thin water layer. The incorporation of the maximum density effect in instability analysis on buoyancy and surface-tension induced cellular convection does not appear to have been considered in the past.

2. FORMULATION OF THE THERMAL INSTABILITY PROBLEM

Following the known procedure for linear stability analysis [10, 14, 15] and referring to the coordinate system shown in Fig. 3, the perturbation equations can be written as

$$\frac{\partial U}{\partial X}+\frac{\partial V}{\partial Y}+\frac{\partial W}{\partial Z}=0 \tag{1}$$

$$\frac{\partial U}{\partial t}=-\frac{1}{\rho_0}\frac{\partial P'}{\partial X}+\nu\nabla^2_{X,Y,Z}U^2 \tag{2}$$

$$\frac{\partial V}{\partial t}=-\frac{1}{\rho_0}\frac{\partial P'}{\partial Y}+\nu\nabla^2_{X,Y,Z}V \tag{3}$$

$$\frac{\partial W}{\partial t}=-\frac{1}{\rho_0}\frac{\partial P'}{\partial Z}+\nu\nabla^2_{X,Y,Z}W-\frac{\delta\rho}{\rho_0}g \tag{4}$$

$$\frac{\partial\theta'}{\partial t}=\tau W+\alpha\nabla^2_{X,Y,Z}\theta' \tag{5}$$

where $\nabla^2_{X,Y,Z}=\partial^2/\partial X^2+\partial^2/\partial Y^2+\partial^2 Z^2$ and the perturbed quantities for temperature, pressure and density are defined by $T=T_b(Z)+\theta'(t,X,Y,Z)$, $P=P_b+P'$, and $\rho=\rho_b+\delta\rho$, respectively. As shown in [12], the boundary conditions at the lower boundary are

$$W=0,\quad \frac{\partial W}{\partial Z}=0 \quad\text{and}\quad \theta'=0 \quad\text{at}\quad Z=0 \tag{6}$$

while at the upper boundary

$$W=0,\quad \rho\nu\frac{\partial^2 W}{\partial Z^2}=\sigma_0\left(\frac{\partial^2\theta'}{\partial X^2}+\frac{\partial^2\theta'}{\partial Y^2}\right)\quad\text{and}$$
$$-K\frac{\partial\theta'}{\partial Z}=q_0\theta' \quad\text{at}\quad Z=d. \tag{7}$$

The density–temperature relationship for water can be approximated by the following equation for the temperature range 0–30°C [10].

$$\rho=\rho_{\max}[1-\gamma_1(T-T_{\max})^2-\gamma_2(T-T_{\max})^3]. \tag{8}$$

Considering the change in the density $\delta\rho$ caused by the temperature perturbation θ', one obtains the following expression after neglecting the terms containing $(\theta')^2$ or higher order.

$$\delta\rho=-\rho_{\max}\left[2\gamma_1(A\Delta T)\left\{1+\frac{3\gamma_2}{2\gamma_1}(A\Delta T)\right\}\right]\times\theta'\left[1+\lambda_1\left(\frac{Z}{d}\right)+\lambda_2\left(\frac{Z}{d}\right)^2\right] \tag{9}$$

where

$$\lambda_1=\left(-\frac{1}{A}\right)\left[\frac{1+3\frac{\gamma_2}{\gamma_1}(A\Delta T)}{1+\frac{3\gamma_2}{2\gamma_1}(A\Delta T)}\right],$$

$$\lambda_2=\left(\frac{1}{A^2}\right)\left[\frac{\frac{3\gamma_2}{2\gamma_1}(A\Delta T)}{1+\frac{3}{2}\frac{\gamma_2}{\gamma_1}(A\Delta T)}\right],$$

$A=(T_1-T_{\max})/\Delta T$ and $\Delta T=T_1-T_2=\tau d$. The thermal parameters λ_1 and λ_2 were first introduced by Sun *et al.* [10].

Introducing the dimensionless variables $(X,Y,Z)=d(x,y,z)$, $(U,V,W)=(\alpha/d)(u,v,w)$, $P'=(\rho_0\alpha\nu/d^2)p$, $\theta'=(\Delta T)\theta$, and eliminating u, v, p by using continuity equation, one obtains the following perturbation equations by assuming the principle of exchange of stability to be valid [10, 15].

$$\nabla^2\nabla^2 w=-Ra(1+\lambda_1 z+\lambda_2 z^2)\nabla_1^2\theta \tag{10}$$

$$\nabla^2\theta=-w \tag{11}$$

where $Ra=g(2\gamma_1 A\Delta T)(\Delta T)d^3[1+(3\gamma_2/2\gamma_1)(A\Delta T)]/(\nu\alpha)$, $\nabla^2=\partial^2/\partial x^2+\partial^2/\partial y^2+\partial^2/\partial z^2$ and $\nabla_1^2=\partial^2/\partial x^2+\partial^2/\partial y^2$. The boundary conditions are

$$w=\frac{\partial w}{\partial z}=\theta=0 \quad\text{at}\quad z=0 \tag{12}$$

$$w=0,\quad \frac{\partial^2 w}{\partial z^2}=Ma\nabla_1^2\theta \quad\text{and}\quad \frac{\partial\theta}{\partial z}=-Bi\theta \quad\text{at}\quad z=1 \tag{13}$$

where $Ma=\sigma_0(\Delta T)d/(\mu\alpha)$ = Marangoni number and $Bi=q_0 d/K$ = Biot number. In contrast to the classical Benard Problem, the onset of convection is possible with heating from below or above because of the presence of $(\Delta T)^2$ in the expression for Rayleigh number. Since restriction is made to the case where instability first appears in the form of cellular convection rather than oscillations associated with overstability, the following normal modes can be assumed for the disturbance quantities.

$$[w,\theta]=[w^+(z),\theta^+(z)]\exp[i(a_1 x+a_2 y)]. \tag{14}$$

Substituting equation (14) into equations (10) and (11), one obtains

$$(D^2-a^2)^2 w^+=a^2 Ra(1+\lambda_1 z+\lambda_2 z^2)\theta^+ \tag{15}$$

$$(D^2-a^2)\theta^+=-w^+. \tag{16}$$

With the boundary conditions

$$w^+=Dw^+=\theta^+=0 \quad\text{at}\quad z=0 \tag{17}$$

$$w^+=0,\quad D^2 w^+=-a^2 Ma\theta^+ \quad\text{and}$$
$$D\theta^+=-Bi\theta^+ \quad\text{at}\quad z=1 \tag{18}$$

where $D=\mathrm{d}/\mathrm{d}z$ and $a=(a_1^2+a_2^2)^{1/2}$ is the wave number of the disturbance. For the limiting case $Ma=0$ and $Bi=\infty$, the present eigenvalue problem reduces to that discussed by Sun *et al.* [10]. When $Ra=0$, the problem reduces to that solved by Pearson [11]. The limiting values $Bi=0$ and ∞ correspond to constant heat flux

and constant temperature and the surface is usually referred to as "insulating" and "thermally conducting" respectively. For given thermal boundary conditions (given λ_1, λ_2 and Bi) and a given Marangoni number Ma, the neutral stability relations give Ra as a function of a and the critical (minimum) Rayleigh number is sought. Conversely when Ra is known, one can determine the critical Marangoni number and the corresponding wavenumber. Apparently, the present problem can be solved by analytical method [10, 12, 15, 16] as well as finite-difference method. The numerical method is preferred in this study since the efficient general finite-difference method is available from the related study [17].

The finite-difference scheme used is due to Thomas [18, 19] and the iterative solution starts with equation (11) by using $w_k^+ = \sin(2\pi k/M)$, $k = 2, \ldots, M$ for the disturbance velocity w^+. The mesh size used is $M = 50$ and a new and improved eigenvalue Ra or Ma is calculated by the following equation [20].

$$(Ra, Ma)_{\text{new}} = (Ra, Ma)_{\text{old}} \left[\sum_k (w_k^+)_{\text{old}}^2\right]^{1/2} / \left[\sum_k (w_k^+)_{\text{new}}^2\right]^{1/2}. \quad (19)$$

The convergence criterion is

$$\sum_k |(w_k^+)_{\text{new}} - (w_k^+)_{\text{old}}| / \sum_k |(w_k^+)_{\text{new}} \leqslant 10^{-6}. \quad (20)$$

It is found that only a few iterations are required to satisfy the above criterion and five significant figures for critical eigenvalue are correct.

3. NUMERICAL RESULTS AND DISCUSSION

Because of the number of parameters involved, only typical numerical results can be presented here. The thermal condition parameters λ_1, λ_2 depend on A as well as $\Delta T = \tau d$. For the temperature range (0–30°C) under consideration, A is always positive and λ_1 is always negative. Furthermore, the temperature coefficient γ_1 (positive) is of order 10^{-5} and λ_2 (negative) is of order 10^{-7}. The expression for λ_2 reveals that λ_2 is negative for heating from below and positive for heating from above. In addition, the unstable liquid layer is always confined to the region near the bottom plate and instability occurs only when $T_1 \geqslant 4$°C for heating from below and when $T_1 < 4$°C for heating from above.

Figures 1 and 2 show neutral stability curves for various cases and the effect of the parameter can be seen clearly. The limiting cases of $Ra = 0$ and $Ma = 0$ corresponds to Pearson problem [11] and Rayleigh problem, respectively. The distributions of eigenfunctions w^+ and θ^+ are shown in Fig. 3 for $Ma = 10$, $\lambda_1 = -1.5$, $\lambda_2 = -0.2$ (heating from below) with Biot number as parameter. It is seen that the curves are quite similar in the lower region up to the location z where the value is maximum. Near the upper free surface, the Biot number effect is quite appreciable, particularly for θ^+. The disturbance profiles for $\lambda_1 = -2$, $\lambda_2 = 0.4$ (heating from above) and $Bi = 100$ are shown in Fig. 4. With $Ma = 0$, the disturbance quantity becomes negative. Otherwise the curves for $Ma = -30$ and -1000 are similar.

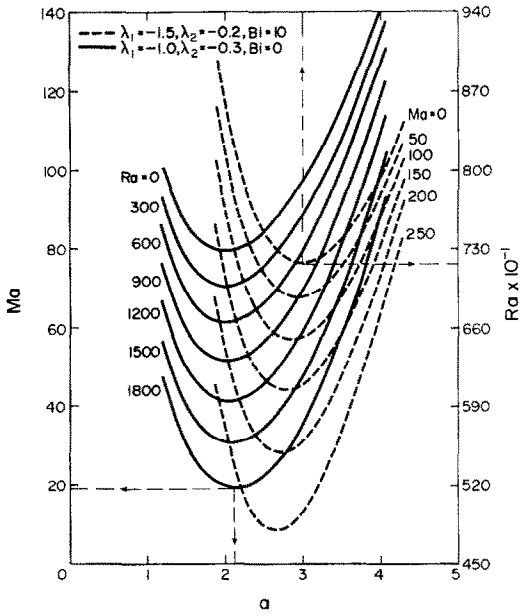

FIG. 1. Neutral stability curves for $\lambda_1 = -1.0$, $\lambda_2 = -0.3$, $Bi = 0$ and $\lambda_1 = -1.5$, $\lambda_2 = -0.2$, $Bi = 10$.

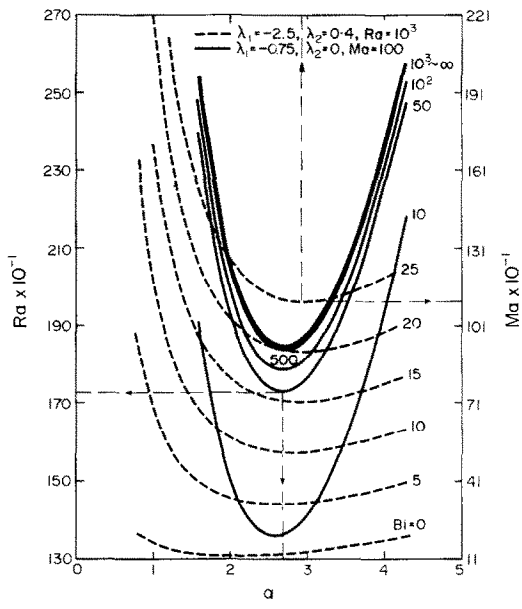

FIG. 2. Neutral stability curves for $\lambda_1 = -0.75$, $\lambda_2 = 0$, $Ma = 10^2$ and $\lambda_1 = -2.5$, $\lambda_2 = 0.4$ and $Ra = 10^3$.

The relation between critical Marangoni number Ma^* and Rayleigh number is shown in Fig. 5 for a range of Biot numbers with $\lambda_1 = -1.5$ and $\lambda_2 = -0.2$ (heating from below). As Bi increases, the critical Marangoni number also increases supporting the physical explanation given in [12] for the case of conducting free surface ($Bi = \infty$). Figure 6 illustrates the variation of the critical Rayleigh number Ra^* with the Marangoni number for a range of Biot numbers with $\lambda_1 = -1.25$ and $\lambda_2 = 0$. The general trend is similar to that shown in Fig. 2 of [13] which corresponds to the limiting case without maximum

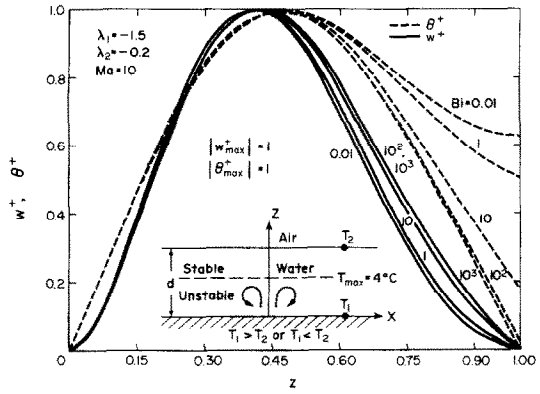

FIG. 3. Coordinate system and disturbance profiles for w^+/w^+_{max} and θ^+/θ^+_{max} for $\lambda_1 = -1.5$, $\lambda_2 = -0.2$, $Ma = 10$ with Bi as parameter.

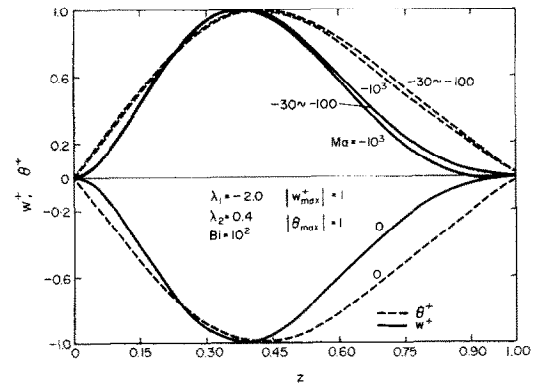

FIG. 4. Disturbance profiles for w^+/w^+_{max} and θ^+/θ^+_{max} for $\lambda_1 = -2.0$, $\lambda_2 = 0.4$, $Bi = 100$ with Ma as parameter.

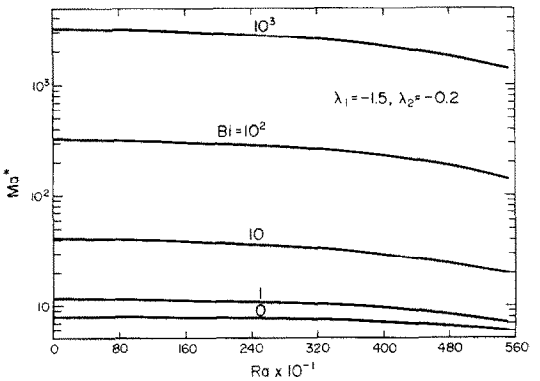

FIG. 5. Relation between critical Marangoni number and Rayleigh number with Bi as parameter for $\lambda_1 = -1.5$ and $\lambda_2 = -0.2$.

density effect. For smaller Biot numbers, the Marangoni effect is seen to be appreciable. As explained in [12], the critical Rayleigh number for a fixed value of Ma is clearly seen to be an increasing function of Bi. The expression for the thermal parameter γ_2 reveals that $\lambda_2 = 0$ when $\gamma_2 = 0$ (parabolic density–temperature relation valid for temperature range $0 \sim 8°C$) or $T_1 = T_{max}$. For given values of Marangoni number, the relation between critical Rayleigh number Ra^* and Biot number is shown in Fig. 7 for $\lambda_1 = -1.5$ and $\lambda_2 = -0.2$ (heating from below). At $Bi = 10^4$, the

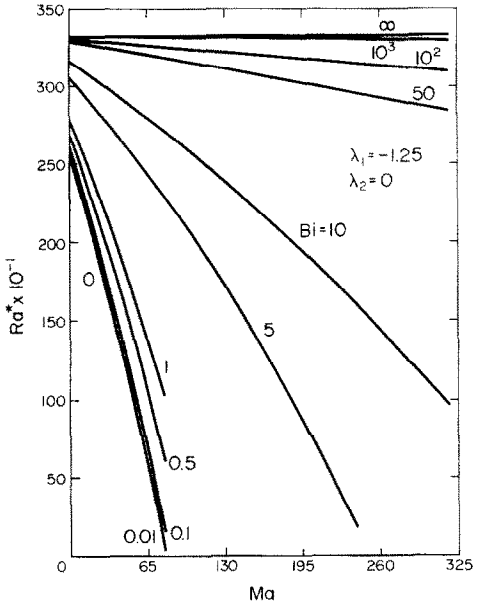

FIG. 6. Relation between critical Rayleigh number and Marangoni number with Bi as parameter for $\lambda_1 = -1.25$ and $\lambda_2 = 0$.

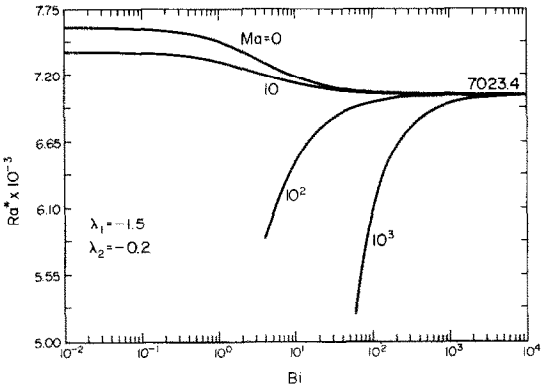

FIG. 7. Relation between critical Rayleigh number and Biot number with Ma as parameter for $\lambda_1 = -1.5$ and $\lambda_2 = -0.2$.

asymptotic value $Ra^* = 7023.4$ is reached. In interpreting the behavior of the curves for $Ma = 100$ and 1000 at the other end, it is useful to note that for a given Marangoni number a critical value of Ra^* does not exist below a certain value of Bi as shown in Fig. 6. Similar plot for the case of heating from above with $\lambda_1 = -2.0$ and $\lambda_2 = 0.4$ is shown in Fig. 8. One also notes the existence of the asymptotic value for Ra^* at $Bi \approx 10^4$. Selected numerical instability results are listed in Tables 1 and 2 for future reference. For the case when buoyancy effects are negligible ($Ra = 0$), the values of the critical Marangoni number and the corresponding wavenumber agree excellently with those listed in [12, 21] for various values of Bi. On the other hand, with $Ma = 0$ and $Bi = 10^4$, the values of $Ra^* = 7023.4$ and $a^* = 2.992$ compare well with $Ra^* = 7027.86$ and $a^* = 2.987$ listed in [22] for $Bi = \infty$. Thus, one may conclude that the present numerical results are sufficiently accurate (five significant figures are correct).

Table 1 Instability Results for $\lambda_1 = -1.5$ and $\lambda_2 = -0.2$

Ra	0		3×10^3		5×10^3		Ma	0		10^2		10^3	
Bi	a*	Ma*	a*	Ma*	a*	Ma*	Bi	a*	Ra*	a*	Ra*	a*	Ra*
0	1.993	79.687	2.054	76.107	2.282	64.023	0	3.137	7587.0				
1	2.246	116.25	2.242	104.41	2.422	82.070	1	3.093	7471.0				
10	2.742	413.92	2.592	339.32	2.652	235.25	4	3.040	7297.4	2.693	5840.2		
10^2	2.975	3307.8	2.722	2642.0	2.732	1745.8	10	3.013	7176.7	2.856	6482.8		
10^3	3.009	32.21×10^3	2.742	25.65×10^3	2.742	16.84×10^3	60	2.995	7056.0	2.967	6923.5	2.774	5203.0
10^4	3.013	32.12×10^4					10^2	2.994	7043.3	2.977	6962.8	2.831	6067.5
							10^3	2.992	7025.3	2.990	7017.1	2.975	6941.8
							10^4	2.992	7023.4	2.991	7022.6	2.990	7015.2

Table 2 Instability Results for $\lambda_1 = -2.0$, $\lambda_2 = 0.4$

Ma	Bi	0.1	1.0	10	10^2	10^3	∞
0	a*	4.603	4.002	3.402	3.332	3.322	3.322
	Ra*	13535	12502	11804	11539	11500	11495
-10^2	a*				3.346	3.324	3.322
	Ra*				11600	11507	11496
-10^3	a*				3.402	3.338	3.322
	Ra*				12059	11565	11496

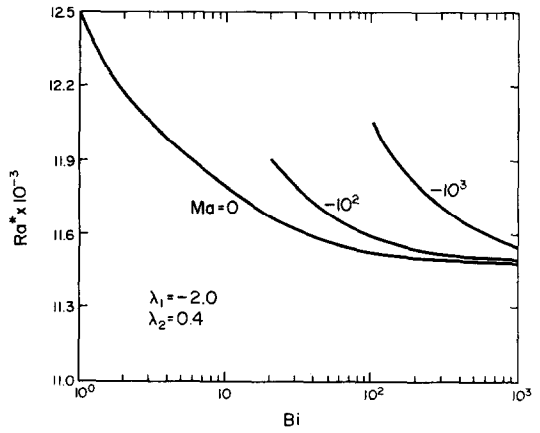

FIG. 8. Relation between critical Rayleigh number and Biot number with Ma as parameter for $\lambda_1 = -2.0$ and $\lambda_2 = 0.4$.

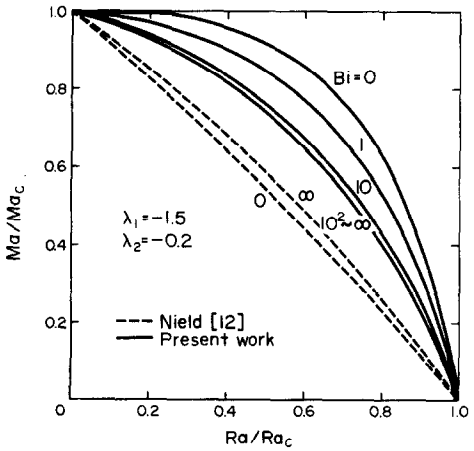

FIG. 9. Variation of normalized Marangoni number Ma/Ma_c with normalized Rayleigh number Ra/Ra_c with Bi as parameter for $\lambda_1 = -1.5$ and $\lambda_2 = -0.2$.

Nield [12, 26] concludes for the case of linear density variation that the coupling between the buoyancy and surface-tension effects is surprisingly tight for all values of Bi and especially tight for $Bi = 0$. It is instructive to compare the present results considering maximum density effects with those shown in Figs. 1 and 2 of [12]. The comparison is shown in Figs. 9 (plot of Marangoni and Rayleigh numbers for marginal stability) and 10 (plot of wavenumber corresponding to marginal stability against normalized Rayleigh number). Figure 9 shows that with maximum density effect the coupling is rather weak and the Biot number effect is characteristically different. Furthermore, Nield's result [12] shows that the form of the relationship between Ma and Ra is a rather weak function of the Biot number but this is not so for the present problem. As noted by Nield [12, 26], the departure of an actual curve from the straight line, $Ra/Ra_c + Ma/Ma_c = 1$, representing perfect coupling, is a measure of the amount of uncoupling. Ra_c is the critical Rayleigh number corresponding to $Ma = 0$ and Ma_c corresponds to $Ra = 0$. In Fig. 10, one sees that when the free surface is "insulating" ($Bi = 0$), the coupling is especially tight for the case of linear density variation [12] but the dimensionless wavenumber for the present problem varies considerably as the value of Ra/Ra_c increases from 0 to 1. Figure 10 also shows that larger cells or smaller wavenumbers are associated with the insulating case $Bi = 0$. At this point, Fig. 3 also supports the observation that with an insulated boundary it is easier for temperature perturbations to be set up [12]. As Bi increases, the corresponding wavenumber increases and the size of the convection cell decreases.

Streamlines in Benard convection cells induced by surface tension and buoyancy are given by Nield [23]. The streamlines in the two vertical planes of symmetry of a hexagonal cell at the onset of convection are shown in Fig. 11(a) and (b) for $\lambda_1 = -1.5$, $\lambda_2 = -0.2$, $Ma = 10$ and $Bi = 100$ by using equations (4) and (5) of [23]. In Fig. 11, the left-hand margin represents the cell boundary and the right-hand margin corresponds to the cell centre. In contrast to the streamline patterns shown in [23], the eyes of the streamlines are seen to be located nearer to the lower rigid plate. Figure 3 also shows that the maximum vertical disturbance w^+ is located nearer to the bottom plate. One notes that for the present problem the unstable layer is situated near the bottom plate.

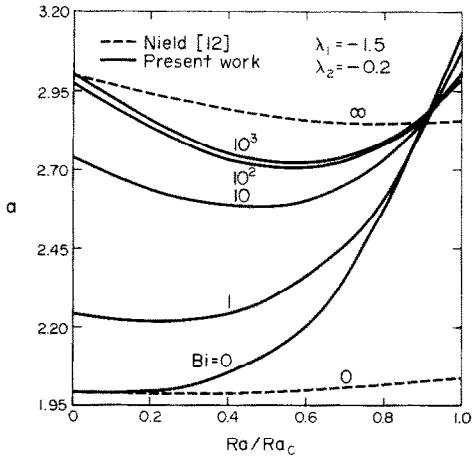

FIG. 10. Variation of dimensionless wavenumber a with normalized Rayleigh number Ra/Ra_c with Bi as parameter for $\lambda_1 = -1.5$ and $\lambda_2 = -0.2$.

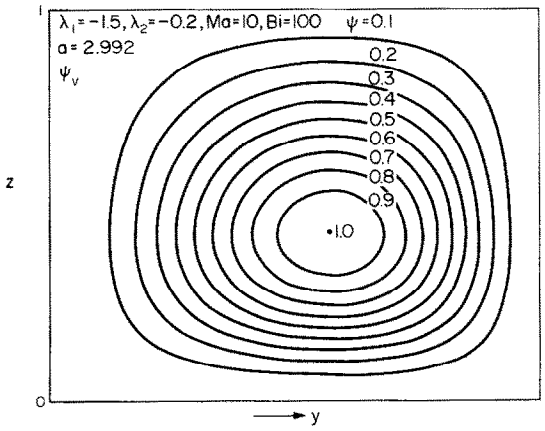

FIG. 11. Streamlines for $\lambda_1 = -1.5$, $\lambda_2 = -0.2$, $Ma = 10$, $Bi = 10^2$, (a) through the center and a vertex of the hexagon, (b) through the center of the hexagon and the mid-point of a side.

4. CONCLUDING REMARKS

1. The physical model [12] assumes that the free upper liquid surface remains undeformed. Nield's linear stability analysis [12] considering surface tension and buoyancy effects has been confirmed by experiments [24, 25]. The limitation of the assumption that departures of the upper surface from a horizontal plane are negligible as well as the possibility for oscillatory instability is well discussed by Nield [26]. Future analysis should include surface viscosity effect and surface deformation pointed out by Scriven and Sternling [27].

2. The case of heating from above may have direct application in surface melting involving ice layer on a lake or pond. The present analysis can be used in predicting the onset of convection for a thin liquid layer on ice driven by surface-tension gradients and buoyancy forces.

3. Within the scope of present study, a full parametric study of the problem is not practical since two thermal condition parameters (λ_1, λ_2) and three flow parameters (Bi, Ra, Ma) appear in the analysis. The graphical results presented are useful in assessing the effects of Bi, Ra and Ma on the onset of instability.

4. The Biot number effect is similar to that discussed in [12]. The detailed physical explanation given in [12] provides further insight into the role of maximum density in the present instability problem.

Acknowledgement—This work was supported by the National Research Council of Canada through grant NRC A1655 and a postgraduate scholarship to R. S. Wu.

REFERENCES

1. D. V. Boger and J. W. Westwater, Effect of buoyancy on the melting and freezing process, *J. Heat Transfer* **89C**, 81–89 (1967).
2. Y. C. Yen, Onset of convection in a layer of water formed by melting ice from below, *Physics Fluids* **11**, 1263–1270 (1968).
3. Y. C. Yen and F. Galea, Onset of convection in a water layer formed continuously by melting ice, *Physics Fluids* **12**, 509–516 (1969).
4. M. Sugawara, S. Fukusako and N. Seki, Experimental studies on the melting of a horizontal ice layer, *Trans. Japan Soc. Mech. Engrs* **40**, 3155–3165 (1974).
5. R. S. Tankin and R. Farhadieh, Effects of thermal convection currents on formation of ice, *Int. J. Heat Mass Transfer* **14**, 953–961 (1971).
6. G. Veronis, Penetrative convection, *Astrophys. J.* **137**, 641–663 (1963).
7. P. H. Roberts, Characteristic value problems posed by differential equations arising in hydrodynamics and hydromagnetics, *J. Math. Anal. Appl.* **1**, 195–214 (1960).
8. W. R. Debler, On the analogy between thermal and rotational hydrodynamic stability, *J. Fluid Mech.* **24**, 165–176 (1966).
9. C. Tien, Thermal instability of a horizontal layer of water near 4°C, *A.I.Ch.E.Jl* **14**, 652–653 (1968).
10. Z. S. Sun, C. Tien and Y. C. Yen, Thermal instability of a horizontal layer of liquid with maximum density, *A.I.Ch.E.Jl* **15**, 910–915 (1969).
11. J. R. A. Pearson, On convection cells induced by surface tension, *J. Fluid Mech.* **4**, 489–500 (1958).
12. D. A. Nield, Surface tension and buoyancy effects in cellular convection, *J. Fluid Mech.* **19**, 341–352 (1964).
13. R. Kobayashi, Instabilität einer von unten erwärmten Flüssigkeitsschicht bei gleichzeitiger Berücksichtigung von Oberflächenspannung und Auftriebskraft, *Z. Angew. Math. Phys.* **18**, 845–851 (1967).

14. A. Pellew and R. V. Southwell, On maintained convective motion in a fluid heated from below, *Proc. R. Soc.* **176A**, 312–343 (1940).
15. Z. S. Sun, C. Tien and Y. C. Yen, Onset of convection in a porous medium containing liquid with a density maximum, *Heat Transfer* 1970, Vol. 4, NC 2.11. Elsevier, Amsterdam (1970).
16. D. A. Nield, Surface tension and buoyancy effects in the cellular convection of an electrically conducting liquid in a magnetic field, *Z. Angew. Math. Phys.* **17**, 131–139 (1966).
17. R. S. Wu and K. C. Cheng, Thermal instability of Blasius flow along horizontal plates, *Int. J. Heat Mass Transfer* To be published.
18. L. H. Thomas, The stability of plane Poiseuille flow, *Phys. Rev.* **91**, 780–783 (1953).
19. T. S. Chen, Hydrodynamic stability of developing flow in a parallel plate channel, Ph.D. Thesis, University of Minnesota (1966).
20. G. E. Forsythe and W. R. Wasow, *Finite-Difference Methods for Partial Differential Equations*, Section 24.8. John Wiley, New York (1960).
21. S. H. Davis, Buoyancy-surface tension instability by the method of energy, *J. Fluid Mech.* **39**, 347–359 (1969).
22. Z. S. Sun, Thermal instability and heat transfer of a horizontal layer of liquid with maximum density and heated from below, M.S. Thesis, Syracuse University, N.Y. (1968).
23. D. A. Nield, Streamlines in Benard convection cells induced by surface tension and buoyancy, *Z. Angew. Math. Phys.* **17**, 226–232 (1966).
24. H. J. Palmer and J. C. Berg, Convective instability in liquid pools heated from below, *J. Fluid Mech.* **47**, 779–787 (1971).
25. E. L. Koschmieder, On convection under an air surface, *J. Fluid Mech.* **30**, 9–15 (1967).
26. D. A. Nield, Convection driven by surface-tension gradients and buoyancy forces, Proc. 2nd Australasian Conf. Hydraulics and Fluid Mech. University of Auckland, C45-56 (1965).
27. L. E. Scriven and C. V. Sternling, On cellular convection driven by surface-tension gradients: effects of mean surface tension and surface viscosity, *J. Fluid Mech.* **19**, 321–340 (1964).

EFFET DE DENSITE MAXIMALE SUR L'INSTABILITE THERMIQUE PRODUITE PAR UNE COMBINAISON DES FORCES DE GRAVITE ET DE LA TENSION SUPERFICIELLE

Résumé—L'étude analytique de stabilité linéaire de Nield (1964), pour une couche horizontale de liquide, qui tient compte de l'effet de la tension superficielle et des forces de gravité, est étendue au cas de l'eau avec effet de densité maximale dans le domaine de températures 0–30°C. Deux paramètres thermiques (λ_1, λ_2) et trois paramètres physiques (*Bi*, *Ra*, *Ma*) interviennent dans l'analyse. On donne les résultats représentatifs des cas qui supposent un chauffage soit par le dessous soit par le dessus.

DER EINFLUSS MAXIMALER DICHTE AUF DIE VON AUFTRIEB UND OBERFLÄCHENSPANNUNG ERZEUGTE THERMISCHE INSTABILITÄT

Zusammenfassung—Die lineare Stabilitätsanalyse von Nield (1964) für eine horizontale Flüssigkeitsschicht unter Berücksichtigung der Oberflächenspannung und der Auftriebseffekte wird erweitert auf den Fall von Wasser mit einem Maximaldichteeffekt für den Temperaturbereich von 0–30°C. In der Analyse erscheinen zwei thermische Parameter (λ_1, λ_2) und drei physikalische Parameter (*Bi*, *Ra*, *Ma*). Für Heizung von unten und von oben werden typische Ergebnisse gebracht.

ВЛИЯНИЕ МАКСИМАЛЬНОЙ ПЛОТНОСТИ НА КОНВЕКТИВНУЮ НЕУСТОЙЧИВОСТЬ ЗА СЧЕТ СОВМЕСТНОГО ДЕЙСТВИЯ ПОДЪЕМНОЙ СИЛЫ И ПОВЕРХНОСТНОГО НАТЯЖЕНИЯ

Аннотация — Линейный анализ Нилда (1964) устойчивости горизонтального слоя жидкости с учетом поверхностного натяжения и эффектов всплывания распространяется на случай воды с максимальной плотностью для диапазона температур 0–30°C. При анализе вводятся два тепловых параметра (λ_1, λ_2) и три физических параметра (*Bi*, *Ra*, *Ma*). Представлены результаты для случаев подогрева снизу и сверху.